# Influence of Metal Coordination on the Mismatch Tolerance of Ligand-Modified PNA Duplexes

**ARTICLE** *in* JOURNAL OF THE AMERICAN CHEMICAL SOCIETY · NOVEMBER 2005

Impact Factor: 12.11 · DOI: 10.1021/ja051336h · Source: PubMed

J|A|C|S
ARTICLES
Published on Web 09/29/2005

# Influence of Metal Coordination on the Mismatch Tolerance of Ligand-Modified PNA Duplexes

Richard M. Watson, Yury A. Skorik, Goutam K. Patra, and Catalina Achim*

*Contribution from the Department of Chemistry, Carnegie Mellon University, 4400 5th Avenue, Pittsburgh, Pennsylvania 15213*

Received March 2, 2005; E-mail: achim@cmu.edu

***Abstract:*** Recent studies on metal incorporation in ligand-modified nucleic acids have focused on the effect of metal coordination on the stability of metal-containing duplexes or triplexes and on the metal binding selectivity but did not address the effect of the sequence of the nucleic acid in which the ligands are incorporated. We have introduced 8-hydroxyquinoline **Q** in 10-mer PNA strands with various sequences and have investigated the properties of the duplexes formed from these strands upon binding of $Cu^{2+}$. Variable-temperature UV−vis spectroscopy shows that, in the presence of $Cu^{2+}$, duplexes are formed even from ligand-modified **Q**−**PNA** strands that have a large number of mismatches. Spectrophotometric titrations demonstrate that at any temperature, one $Cu^{2+}$ ion binds a pair of **Q**−**PNA** strands that each contain one 8-hydroxyquinoline, but below the melting temperature, the PNA duplex exerts a supramolecular chelate effect, which prevents the transformation in the presence of excess $Cu^{2+}$ of the 1:2 $Cu^{2+}$:**Q**−**PNA** complexes into 1:1 complexes. EPR spectroscopy gives further support for the existence in the duplexes of [Cu$\mathbf{Q}_2$] moieties that are similar to the corresponding square planar synthetic complex formed between $Cu^{2+}$ and 8-hydroxyquinoline. As PNA duplexes show a preferred handedness due to the chiral induction effect of a C-terminal L-lysine, which is transmitted through stacking interactions within the duplex, only if the metal-containing duplex has complementary strands, does it show a chiral excess measured by CD spectroscopy. The strong effect of the metal−ligand moiety is suggestive of an increased correlation length in PNA duplexes that contain such moieties. These results indicate that strong metal−ligand alternative base pairs significantly diminish the importance of Watson−Crick base pairing for the formation of a stable PNA duplex and lead to high mismatch tolerance, a principle that can be used in the construction of hybrid inorganic−nucleic acid nanostructures.

## Introduction

Metal ions play important roles in the structure and function of nucleic acids, and numerous modified nucleic acids that bind transition metal ions are presently being used for diagnostic and therapeutic applications. As a consequence, the effects of metal binding to backbone phosphates or nucleobases on DNA properties have been extensively investigated.[1−4] Eichhorn et al. have studied the effect of transition metal ions, in particular of $Cu^{2+}$, on DNA structure and stability, and they have determined that in solutions containing at least one $Cu^{2+}$ equivalent per DNA base pair, $Cu^{2+}$ binds to nucleobases at high temperature, decreases significantly the thermal stability of DNA duplexes, and can prevent DNA hybridization upon cooling.[5−7] In the presence of less than 0.4 equiv of $Cu^{2+}$ per DNA base pair, the thermal stability of DNA was found to slightly increase, an effect attributed to possible $Cu^{2+}$ binding to the phosphate backbone.[5]

Besides their biological functions, nucleic acids' ability to store and transmit information has been recently exploited for the creation of nanostructures and molecular electronics devices.[8−10] Incorporation of transition metal ions into these systems is a means to expand the range of electronic and magnetic properties of the nanostructures. Furthermore, the combined use of the hybridization properties of nucleic acids and coordination properties of the metal ions offers an opportunity to create hybrid nucleic−acid structures with new topologies. Transition metal ions can be incorporated into nucleic acids by substitution of the natural nucleobases with ligands. In the presence of metal ions, these ligand-containing nucleic acids form supramolecular structures based on a combination of coordination and hydrogen bonds. This strategy has been successfully applied in the last 5 years to introduce $Ni^{2+}$, $Cu^{2+}$, and $Ag^{+}$ in DNA duplexes and triplexes.[11−19] Recently, we have extended this approach to incorporation of

(1) Barton, J. K.; Lippard, S. J. *Metal Ions Biol.* **1980**, *1*, 31−113.
(2) Houlton, A. *Adv. Inorg. Chem.* **2002**, *53*, 87−158.
(3) Lippert, B. *Coord. Chem. Rev.* **2000**, *200*−*202*, 487−516.
(4) Derose, V. J.; Burns, S.; Kim, N. K.; Vogt, M. *Compr. Coord. Chem. II* **2004**, *8*, 787−813.
(5) Eichhorn, G. L.; Clark, P. *Proc. Natl. Acad. Sci. U.S.A.* **1965**, *53*, 586−593.
(6) Eichhorn, G. L.; Shin, Y. A. *J. Am. Chem. Soc.* **1968**, *90*, 7323−7328.
(7) Eichhorn, G. L.; Rifkind, J. M.; Shin, Y. A. *Adv. Chem. Ser.* **1977**, *162*, 304−311.
(8) Seeman, N. C. *Trends Biochem. Sci.* **2005**, *30*, 119−125.
(9) Seeman, N. C.; Lukeman, P. S. *Rep. Prog. Phys.* **2005**, *68*, 237−270.
(10) Braun, E.; Keren, K. *Adv. Phys.* **2004**, *53*, 441−496.
(11) Shionoya, M.; Tanaka, K. *Curr. Opin. Chem. Biol.* **2004**, *8*, 592−597.
(12) Shionoya, M.; Tanaka, K. *Bull. Chem. Soc. Jpn.* **2000**, *73*, 1945−1954.
(13) Meggers, E.; Holland, P. L.; Tolman, W. B.; Romesberg, F. E.; Schultz, P. G. *J. Am. Chem. Soc.* **2000**, *122*, 10714−10715.
(14) Zhang, L.; Meggers, E. *J. Am. Chem. Soc.* **2005**, *127*, 74−75.
(15) Zimmermann, N.; Meggers, E.; Schultz, P. G. *Bioorg. Chem.* **2004**, *32*, 13−25.


**10.1021/ja051336h CCC: $30.25** 

$Ni^{2+}$ into peptide nucleic acid (PNA) duplexes by replacing two complementary nucleobases with two bipyridine moieties.[20,21]

The properties of these metal-containing supramolecular assemblies depend on both the nucleic acid part and the metal−ligand moiety but are not simply the sum of their properties. For example, replacement of two complementary bases with two ligands that cannot form hydrogen bonds leads to destabilization of the nucleic acid duplexes, with the destabilization being more pronounced for PNA than for DNA duplexes, in a manner similar to the better mismatch discrimination of PNA when compared to DNA. When metal ions are present, the duplex stabilization is partly or completely restored, as expected because coordination bonds are formed in these structures. As these bonds are stronger than hydrogen bonds, the fact that in some cases the thermal stability of the metal-containing duplexes is lower than that of the nonmodified duplexes indicates that other factors, such as steric interactions that weaken hydrogen bonds in, and $\pi-\pi$ stacking interactions between, nucleobase pairs adjacent to the metal-bridged ligand pair, play an important role in determining the properties of the duplexes.

Predictions of the duplex properties based on coordination chemistry concepts do not hold in a consistent fashion. For example, Schultz et al. have introduced in DNA duplexes the monodentate ligand pyridine and either pyridine-2,6-dicarboxylate to create a [1+3] binding site for $Cu^{2+}$ or 2,6-bis(ethylthiomethyl)pyridine to create a [1+3] binding site for the softer $Ag^+$.[13,16] $Cu^{2+}$ incorporation occurred and had a predictable effect on a DNA duplex containing the former ligand combination, but surprisingly, in the presence of $Ag^+$, DNA duplexes with the latter ligand combination had thermal stability slightly lower than that of nonmodified duplexes. Also, significantly more stable duplexes were formed when two tridentate 2,6-bis(ethylthiomethyl)pyridine ligands were present in complementary positions in the DNA duplex, suggesting a six-coordinate $Ag^+$ complex, which is unusual. Furthermore, comparison between results obtained for pyridine-modified DNA duplexes that have different sequences indicates a context dependent effect of the metal−ligand moiety on the duplex properties.[16,22]

During the study of metal incorporation in PNA duplexes, we have found that the stability of a 2,2′-bipyridine-modified PNA duplex in the presence of $Ni^{2+}$ is lower than that of a duplex that has an AT base pair.[20] This observation may be attributed to the fact that in a four-coordinate bis(bipyridine) metal complex, the two ligands cannot be coplanar due to steric interactions between protons situated in the 6 and 6′ positions. As a consequence, square planar complexes undergo a tetrahedral distortion, with the two ligands being twisted, or adopt a bow-step conformation in which the two ligands are situated in off-set parallel planes.[23] These distortions potentially interfere with the formation of hydrogen bonds within the base pairs adjacent to the metal−ligand pair and reduce $\pi$-stacking, and thus have a destabilization effect on the duplex.

To test this hypothesis, 8-hydroxyquinoline (**Q**) has been introduced into PNA oligomers (**Q**−**PNA**), and the properties of duplexes formed by these oligomers in the presence of $Cu^{2+}$ have been investigated. As a synthetic complex [Cu$\mathbf{Q}_2$] is known and its square planar geometry is well documented,[24−27] we anticipated that the $Cu^{2+}$-containing PNA duplexes would have higher thermal stability than the nonmodified PNA. This paper presents the results of the study of 10-mer **Q**−PNA oligomers in the presence of $Cu^{2+}$ using UV−vis, CD, and EPR spectroscopy. While this work was in progress, Zhang et al. have shown that the formation of a 15 base pair DNA duplex that contains in the middle of the duplex, in complementary positions, two **Q** ligands leads in the presence of $Cu^{2+}$ to formation of very stable DNA duplexes and makes possible modifications of the DNA backbone that would otherwise prevent the duplex assembly.[14] In the present study, we show that strong metal binding to 8-hydroxyquinoline ligands within two PNA oligomers promotes the formation of a PNA duplex even when several mismatches exist between the two strands, a result which suggests an important role of metal coordination in the stabilization of peptide nucleic acid structures.

## Experimental Section

**Materials.** *tert*-Butyl *N*-(2-Boc-aminoethyl)-glycinate **2** was prepared according to a published procedure.[28] The 5-carboxymethyl-8-hydroxyquinoline **3** was prepared as shown in Scheme 1, using literature procedures for steps a−c.[29,30]

***Scheme 1*** [a]

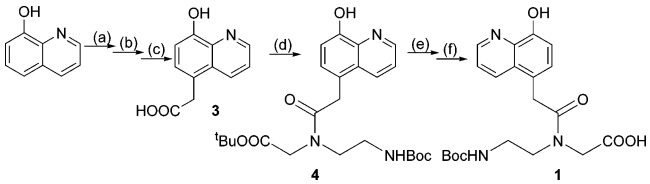


[a] (a) HCl, formaldehyde; (b) NaCN, DMSO, 90 °C; (c) HCl; (d) **2**, DCC, DhbtOH; (e) NaOH, MeOH; (f) HCl.

All other reagents were obtained from commercially available sources, were of analytical grade quality, and were used without further purification. Silica gel for column chromatography was 200−400 mesh size. All reactions were monitored by TLC on $SiO_2$ (UV detection). Melting points were measured using a Mel-Temp II instrument and are uncorrected. Elemental analysis was done by Prevalere Life Sciences, Inc. $^1$H NMR spectra were recorded on a Bruker Cryospec WM 300. A Finnegan Mattson instrument was used for electrospray mass spectrometry (ES-MS).

***tert*-Butyl-2-(*N*-(*tert*-butyloxycarbonyl-2-aminoethyl)-2-(8-hydroxyquinoline-5-yl)acetamido) Acetate (4).** 0.82 g (3 mmol) of **2** was dissolved in 15 mL of DCM. To this solution were added 0.49 g (3 mmol) of DhbtOH and 0.72 g (3 mmol) of **3**·HCl dissolved in 20 mL of DMF (by slight warming). The reaction mixture was cooled to

(16) Zimmermann, N.; Meggers, E.; Schultz, P. G. *J. Am. Chem. Soc.* **2002**, *124*, 13684−13685.
(17) Weizman, H.; Tor, Y. *J. Am. Chem. Soc.* **2001**, *123*, 3375−3376.
(18) Switzer, C.; Shin, D. *Chem. Commun.* **2005**, 1342−1344.
(19) Switzer, C.; Sinha, S.; Kim, P. H.; Heuberger, B. D. *Angew. Chem., Int. Ed.* **2005**, *44*, 1529−1532.
(20) Popescu, D.-L.; Parolin, T. J.; Achim, C. *J. Am. Chem. Soc.* **2003**, *125*, 6354−6355.
(21) Franzini, R.; Watson, R. M.; Popescu, D.-L.; Patra, G. K.; Achim, C. *Polym. Prepr.* **2004**, *45*, 337−338.
(22) Tanaka, K.; Yamada, Y.; Shionoya, M. *J. Am. Chem. Soc.* **2002**, *124*, 8802−8803.
(23) Geremia, S.; Randaccio, L.; Mestroni, G.; Milani, B. *J. Chem. Soc., Dalton Trans.* **1992**, 2117−2118 and references therein.
(24) Ammor, S.; Coquerel, G.; Perez, G.; Robert, F. *Eur. J. Solid State Inorg. Chem.* **1992**, *29*, 445.
(25) Bevan, J. A.; Graddon, D. P.; McConnell, J. F. *Nature* **1963**, *199*, 373.
(26) Hoy, R. C.; Morriss, R. H. *Acta Crystallogr.* **1967**, *22*, 476−482.
(27) Murray-Rust, P.; Wright, J. D. *J. Chem. Soc. A* **1968**, 247−253.
(28) Dueholm, K. L.; Egholm, M.; Behrens, C.; Christensen, L.; Hansen, H. F.; Vulpius, T.; Petersen, K. H.; Berg, R. H.; Nielsen, P. E.; Buchardt, O. *J. Org. Chem.* **1994**, *59*, 5767−5773.
(29) Burckhalter, J. H.; Leib, R. I. *J. Org. Chem.* **1961**, *26*, 4078−4083.
(30) Warner, V. D.; Sane, J. N.; Mirth, D. B.; Turesky, S. S.; Soloway, B. *J. Med. Chem.* **1976**, *19*, 167−169.

0 °C, and 0.62 g (3 mmol) of solid DCC was added. The solution was stirred vigorously at 0 °C for 2 h. The reaction mixture was then allowed to reach room temperature and was stirred for another 2 h. The finely powdered white precipitate of dicyclohexyl urea (DCU) was removed by filtration. 75 mL of DCM was added to the filtrate. The resulting DCM solution was washed successively with dilute aqueous $NaHCO_3$ (3 × 25 mL), dilute aqueous $KHSO_4$ (2 × 25 mL), and finally with brine (2 × 30 mL). The organic phase was dried over anhydrous $Na_2SO_4$, filtered, and the solvent was evaporated. The solid product obtained after evaporation was redissolved in 10 mL of ethyl acetate. A small amount of white solid DCU, which remained undissolved, was filtered out. The ethyl acetate solution was evaporated to obtain **4** as yellow solid. Yield, 0.798 g (58%). $^1$H NMR (300 MHz, in $CDCl_3$): $\delta$, 8.76 (d, 1H, $H^2$); 8.36 (d, 1H, $H^4$); 7.48 (dd, 1H, $H^3$); 7.35 (d, 1H, $H^6$); 7.10 (d, 1H, $H^7$); 5.47 (m br, NH, 1H); 4.05 (s, 2H, N−$CH_2$−CO); 3.90 (s, 2H, **Q**−$CH_2$); 3.55 (t, 2H, $CH_2$−N═); 3.28 (t, 2H, $CH_2$−NHBoc); 1.40 (m, 18H, Boc + OtBu). ES-MS for $(M + H)^+$ ($CH_3CN$): $m/z$ = 459.93 observed, 460.24 calculated.

**2-(*N*-(*tert*-Butyloxycarbonyl-2-aminoethyl)-2-(8-hydroxyquinolin-5-yl)acetamido) Acetic Acid (1).** Ester **4** (0.918 g, 2 mmol) was dissolved in 10 mL of ethanol. 20 mL water was added to this solution, followed by dropwise addition of 1.5 mL of 12 M aqueous NaOH solution with stirring. The reaction mixture was stirred at room temperature for 4 h. The resulting solution was then filtered, acidified to pH 3 by addition of 4 M HCl, and extracted with 3 × 50 mL ethyl acetate. The ethyl acetate fractions were combined, dried over anhydrous $Na_2SO_4$, filtered, and the solvent was evaporated under vacuum. The hydrolyzed monomer was obtained as a light green solid after being dried under vacuum overnight. Yield, 0.61 g (76%); mp 114−118 °C. Anal. Calcd for $C_{20}H_{25}N_3O_6$: C, 59.54; H, 6.25%. Found: C, 59.17; H, 6.47%. $^1$H NMR (300 MHz, in $CDCl_3$): $\delta$, 8.84 (d, 1H, $H^2$); 8.29 (d, 1H, $H^4$); 7.56 (dd, 1H, $H^3$); 7.30 (d, 1H, $H^6$); 7.01 (d, 1H, $H^7$); 4.28 (s, 2H, N−$CH_2$−CO); 3.97 (s, 2H, **Q**−$CH_2$); 3.53 (t, 2H, $CH_2$−N═); 3.11(t, 2H, C**H$_2$**−NHBoc); 1.37 (m, 9H, Boc). ES-MS for $(M - H)^-$ ($CH_3CN$): $m/z$ = 402.07 observed, 402.17 calculated.

**Solid-Phase PNA Synthesis.** PNA oligomers were synthesized using the Boc-protection strategy.[31] PNA monomers were purchased from Applied Biosystems and used without further purification. After cleavage, PNA was precipitated using ethyl ether and was purified by reversed-phase HPLC using a C18 silica column on a Waters 600 Controller and Pump. Absorbance was measured with a Waters 2996 Photodiode Array Detector. Characterization of the oligomers was performed by MALDI-ToF mass spectrometry on an Applied Biosystems Voyager Biospectrometry Workstation with Delayed Extraction and an α-cyano-4-hydroxycinnamic acid matrix (10 mg/mL in 1:1 water:acetonitrile, 0.1% TFA). MALDI-TOF calcd/found for $(\mathbf{X}_i + H)^+$ $m/z$ $\mathbf{X_A}$ 2855.8/2855.3, $\mathbf{X_B}$ 2855.8/2855.2, **Q**−$\mathbf{X_A}$ 2865.8/2866.0, **Q**−$\mathbf{X_B}$ 2874.8/2875.0, **Q**−$\mathbf{X_C}$ 2865.8/2866.3, **Q**−$\mathbf{X_D}$ 2865.8/2866.4, **Q**−$\mathbf{X_E}$ 2812.9/2813.0, **G**−$\mathbf{X_A}$ 2871.8/2872.0.

**Physical Methods. CD Spectroscopy.** CD spectra were measured for 20 $\mu$M total PNA concentration in pH 7.0 10 mM sodium phosphate buffer solutions. In the case where complementary PNA strands were used, solutions were equimolar in the two strands. CD measurements were conducted on a JASCO J-715 spectropolarimeter equipped with a thermoelectrically controlled, single-cell holder. CD thermal denaturation curves were measured using response time 16 s, sensitivity 20 mdeg, and bandwidth 5.0 nm. The temperature was changed at a rate of 1 °C/min, and data were collected every 0.5 °C. CD spectra were collected using bandwidth 1 nm, response time 1 s, speed 50 nm/min, sensitivity 20 mdeg, and scan accumulation 16.

**UV−Vis Spectroscopy.** UV−vis experiments were performed on a Varian Cary 3 spectrophotometer with programmable temperature block, in 10 mm quartz cells. PNA stock solutions were prepared with nanopure water and were stored at −18 °C. The concentration of PNA oligomers was determined by UV absorption at 95 °C using the sum of the extinction coefficients of the constituent nucleosides $\epsilon_{260}$ taken from the literature.[32] The extinction coefficient for 8-hydroxyquinoline $\epsilon_{260}$ = 2570 ± 110 $M^{-1}$ $cm^{-1}$ (pH = 7.0) was determined from the slope of the calibration curve $A_{260}$ versus concentration. PNA solutions for melting curves and titrations had concentrations in the micromolar range (10−50) and were prepared in pH 7.0 10 mM phosphate buffer. UV−vis titrations were carried out by addition of standard 0.5−2 mM $CuCl_2$ solutions in water to PNA solutions. The absorbance $A$ after each addition was corrected ($A_{corr}$) for dilution and for the contribution of $CuCl_2$ and PNA.

UV melting curves were recorded in the temperature range 5−95 °C for both cooling and heating modes, at the rate of 1 °C/min. Prior to the measurement of the melting profiles, the solutions were kept at 95 °C for at least 10 min. The difference between the high- and low-temperature spectra of **Q**-modified PNA oligomers in the absence of $Cu^{2+}$ indicates that the maximum absorbance changes induced by temperature occur at 240−244 nm and at 266−270 nm. In the presence of $Cu^{2+}$, the maximum absorbance change occurs at 262−267 nm. Therefore, melting curves were measured at wavelengths within these intervals. $T_m$ is the inflection point of a sigmoidal function used to fit the melting curve.

**EPR Spectroscopy.** EPR spectra were recorded on an X-band (9 GHz) Bruker ESP 300 spectrometer equipped with an Oxford ESR 910 cryostat. The microwave frequency was calibrated with a frequency counter and the magnetic field with a NMR gaussmeter. The temperature was calibrated using devices from Lake Shore Cryonics. Spectra were collected under nonsaturating conditions. Samples were prepared in pH 7.0 10 mM sodium phosphate buffer with 25% glycerol as glassing agent. Samples containing PNA and $Cu^{2+}$ in appropriate molar ratio were heated at 95 °C for 10 min, slowly cooled to room temperature, and then transferred into EPR tubes and frozen. EPR spectra were simulated using the program SpinCount written by Prof. Michael P. Hendrich.[33] Spin quantitation was done relative to a 0.499 mM $Na_2$[Cu(edta)] standard, the copper concentration of which was determined by plasma emission spectroscopy.

## Results

**Synthesis of 8-Hydroxyquinoline−PNA.** The 8-hydroxyquinoline PNA monomer was prepared by coupling the acetic acid derivative of 8-hydroxyquinoline **3** activated using DCC and DhbtOH to the Boc-protected, *tert*-butyl aminoethyl glycinate **2**. In contrast to typical PNA monomer synthesis in which an excess of the acetic acid derivative is used in this coupling step, we have used a stoichiometric amount of **3** to minimize the risk that the phenolic group of **3** reacts with the secondary amino group of **2**. Next, the *tert*-butyl ester **4** obtained from the coupling was hydrolyzed using a dilute sodium hydroxide solution in water/ethanol. The 8-hydroxyquinoline PNA monomer **1** was incorporated into PNA oligomers using solid-phase peptide synthesis based on a Boc-protecting group strategy.[31]

**PNA Sequences.** The antiparallel PNA duplex $\mathbf{X_A}$:$\mathbf{X_B}$ (a in Chart 1) formed by complementary Watson−Crick base pairing of all of its 20 bases has been extensively investigated since PNA's discovery in 1991.[34,35] One A and T nucleobase in the

(31) Christensen, L.; Fitzpatrick, R.; Gildea, B.; Petersen, K. H.; Hansen, H. F.; Koch, T.; Egholm, M.; Buchardt, O.; Nielsen, P. E. *J. Pept. Sci.* **1995**, *1*, 175−183.

(32) Nielsen, P. E., Egholm, M., Eds. *Peptide Nucleic Acid: Protocols and Applications*; Horizon Scientific Press: Wymondham, UK, 1999.

(33) Hendrich, M. P.; Petasis, D.; Arciero, D. M.; Hooper, A. B. *J. Am. Chem. Soc.* **2001**, *123*, 2997−3005.

(34) Wittung, P.; Nielsen, P. E.; Buchardt, O.; Egholm, M.; Norden, B. *Nature* **1994**, *368*, 561−563.

(35) Egholm, M.; Buchardt, O.; Christensen, L.; Behrens, C.; Freier, S. M.; Driver, D. A.; Berg, R. H.; Kim, S. K.; Norden, B.; Nielsen, P. E. *Nature* **1993**, *365*, 566−568.

***Chart 1.*** PNA Sequences and Duplexes[a]

1 2 3 4 5 6 7 8 9 10

$X_A$ H–GTAG**A**TCACT–Lys-$NH_2$ (a)

$X_B$ $H_2N$-Lys–CATC**T**AGTGA–H

10 9 8 7 6 5 4 3 2 1

Q-$X_A$ H–GTAG**Q**TCACT–Lys-$NH_2$ (b)

Q-$X_B$ $H_2N$-Lys–CATC**Q**AGTGA–H

Q-$X_A$ H–GTAG**Q**TCACT–Lys-$NH_2$ (c)

Q-$X_A$ $H_2N$-Lys–TCAC**T**Q**G**ATG–H

Q-$X_B$ H–AGTGA**Q**CTAC–Lys-$NH_2$ (d)

Q-$X_B$ $H_2N$-Lys–CATC**Q**AGTGA–H

Q-$X_C$ H–TGAG**Q**TCACT–Lys-$NH_2$ (e)

Q-$X_C$ $H_2N$-Lys–TCAC**T**Q**G**AGT–H

Q-$X_D$ H–TGAC**Q**TGACT–Lys-$NH_2$ (f)

Q-$X_D$ $H_2N$-Lys–TCAGT**Q**CAGT–H

Q-$X_E$ H–ACAC**Q**ACACA–Lys-$NH_2$ (g)

Q-$X_E$ $H_2N$-Lys–ACACA**Q**CACA–H

G-$X_A$ H–GTAG**G**TCACT–Lys-$NH_2$ (h)

G-$X_A$ $H_2N$-Lys–TCAC**T**G**G**ATG–H

[a] Watson–Crick and wobble base pairs are represented in blue and green, respectively. Alignment of the strands within the duplexes is such that either the **Q** ligands are in complementary position or the number of Watson–Crick base pairs is maxim.

middle of each of the PNA 10-mers $\mathbf{X_A}$ and $\mathbf{X_B}$, respectively, has been replaced by 8-hydroxyquinoline ligands such that in the duplex formed by the modified strands $\mathbf{Q-X_A}$ and $\mathbf{Q-X_B}$, the two ligands are situated in complementary positions (b in Chart 1).

To investigate the synergy between hydrogen and coordination bonds on PNA duplex formation and stability, we have also studied the properties of **Q**-modified PNA 10-mer strands that are partly or non-self-complementary. $\mathbf{Q-X_A}$ and $\mathbf{Q-X_B}$ can form antiparallel homoduplexes $(\mathbf{Q-X_i}:\mathbf{Q-X_i})-Cu^{2+}$ stabilized by four Watson–Crick base pairs and two GT wobble base pairs (c and d in Chart 1). $\mathbf{Q-X_C}$ and $\mathbf{Q-X_D}$ can also form homoduplexes $(\mathbf{Q-X_i}:\mathbf{Q-X_i})-Cu^{2+}$ that contain up to six and four Watson–Crick base pairs, respectively (Chart 2). To investigate the effect of copper on completely noncomplementary **Q–PNA** strands, we have also synthesized the 10-mer $\mathbf{Q-X_E}$, which contains alternating A and C bases that are size complementary but cannot form Watson–Crick base pairs (g in Chart 1).

**Variable-Temperature UV–Vis Spectroscopy.** As mentioned above, substitution of GC or AT base pairs with ligands that cannot form hydrogen bonds generally leads to destabilization of nucleic acid duplexes, while metal binding to these ligand-modified duplexes can partly or completely restore the thermal stability. Variable-temperature UV–vis spectroscopy was used to evaluate changes in the stability of our PNA duplexes upon 8-hydroxyquinoline incorporation and $Cu^{2+}$ binding.

Analysis of the melting curve for the complementary duplex $\mathbf{Q-X_A}:\mathbf{Q-X_B}$ in the absence of $Cu^{2+}$ (Figure 1a), which displays a sigmoidal shape indicative of cooperativity, gives $T_m = 46$ °C, which is 21 °C less than the $T_m$ of the nonmodified $\mathbf{X_A}:\mathbf{X_B}$.[34] In the presence of less than 1 equiv of $Cu^{2+}$ per duplex, two transitions are clearly observable in the melting curves for $\mathbf{Q-X_A}:\mathbf{Q-X_B}$ (Figure 1a): one at ~46 °C, attributed to melting of the metal-free duplex, and one at >79 °C, attributed to melting of the metal-containing duplex. The latter melting temperature represents a lower limit as the transition is not complete up to 95 °C. The relative contribution of the two transitions correlates with the amount of $Cu^{2+}$ present in solution, and at ratios $Cu^{2+}:(\mathbf{Q-X_A}:\mathbf{Q-X_B}) \geq 1:1$, the lower temperature transition disappears and only the transition with $T_m > 79$ °C is observed. The large stabilization of the **Q**-containing duplex upon $Cu^{2+}$ addition ($\Delta T_m > 33$ °C) is in contrast to the nonmodified $\mathbf{X_A}:\mathbf{X_B}$ duplex for which $Cu^{2+}$ addition leads to a very small decrease in $T_m$ ($\Delta T_m = 2$ °C).

Surprisingly, in the presence of $Cu^{2+}$, homoduplexes formed from **Q–PNA** strands that are only partly complementary show a cooperative transition with considerable hyperchromicity (Figure 1b and Table 1). The melting temperatures for homoduplexes based on $\mathbf{Q-X_A}$, $\mathbf{Q-X_B}$, $\mathbf{Q-X_C}$, and $\mathbf{Q-X_D}$ are 72, >79, 77, and 66 °C, respectively. To determine whether the change in absorption with temperature is due to the $[Cu\mathbf{Q}_2]$ moiety situated within the duplex, we have monitored the absorption of a solution containing 5 $\mu$M $Cu^{2+}$ and 10 $\mu$M 8-hydroxyquinoline PNA monomer **1** (Figure S1). We have found that the changes in absorption of this solution with the temperature are linear and significantly smaller ($\Delta A_{267} = 0.03$) than those measured for **Q–PNA** in the presence of $Cu^{2+}$ ($\Delta A_{267} = 0.20$). This experiment established that the changes in absorbance at 267 nm for **Q–PNA** solutions in the presence of $Cu^{2+}$ are indeed due to PNA duplex formation rather than to the $Cu\mathbf{Q}_2$ moiety.

Having observed the formation of duplexes even from partly complementary strands, we have measured the temperature dependence of the absorption at 267 nm for PNA oligomer $\mathbf{Q-X_E}$, which cannot form a homoduplex containing Watson–Crick base pairs. Changes in absorbance for this oligomer in the presence of $Cu^{2+}$ are noncooperative, indicating that a duplex is not formed (Figure 1b).

These results indicate that strong binding of $Cu^{2+}$ to the **Q** ligands in the PNA oligomers leads to high mismatch tolerance,

***Chart 2.*** Alternative Alignments for $(\mathbf{Q-X_C}:\mathbf{Q-X_C})-Cu^{2+}$ and $(\mathbf{Q-X_D}:\mathbf{Q-X_D})-Cu^{2+}$, Which Make Possible the Formation of Watson–Crick Base Pairs[a]

Q-$X_C$ H-TGAG**Q**TCACT-Lys-$NH_2$ Q-$X_D$ H-TGAC**Q**TGACT-Lys-$NH_2$

Q-$X_C$ $H_2N$-Lys-TCACT**Q**GAGT-H Q-$X_D$ $H_2N$-Lys-TCAGT**Q**CAGT-H

Q-$X_C$ H-TGAG**Q**TCACT-Lys-$NH_2$ Q-$X_D$ H-TGACT**Q**GACT-Lys-$NH_2$

Q-$X_C$ $H_2N$-Lys-TCACT**Q**GAGT-H Q-$X_D$ $H_2N$-Lys-TCAG**Q**TCAGT-H

[a] Watson–Crick base pairs are represented in blue.

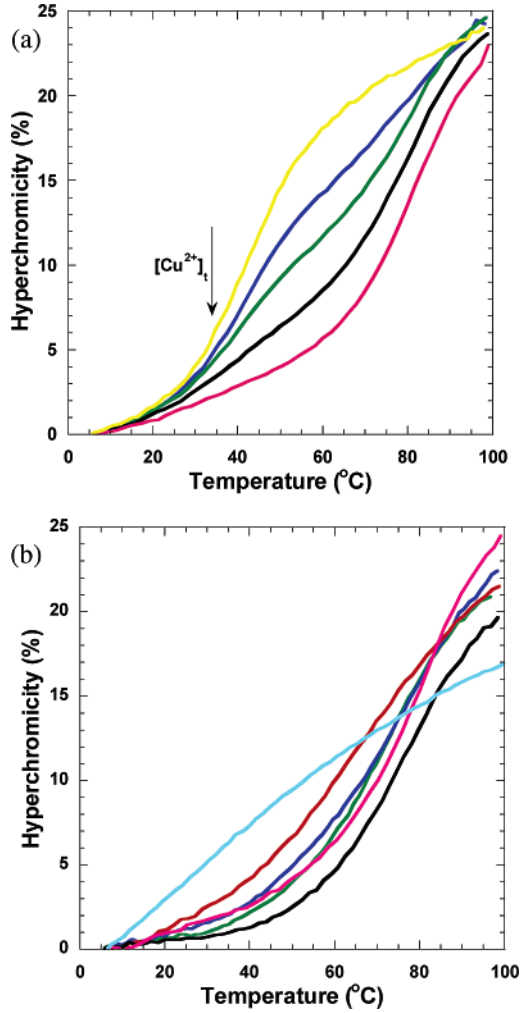


***Figure 1.*** (a) Absorbance change at 267 nm for 5 $\mu$M **Q**−**X$_A$**:**Q**−**X$_B$** solutions in the absence and presence of $CuC1_2$. Concentration of $CuCl_2$: 0, 1, 2, 3, 5 $\mu$M; (b) Absorbance change at 267 nm for 10 $\mu$M **Q**−**PNA** pH = 7.0 10 mM phosphate buffer solutions in the presence of 5 $\mu$M $Cu^{2+}$. **Q**−**X$_A$** (green); **Q**−**X$_B$** (blue); **Q**−**X$_C$** (black); **Q**−**X$_D$** (red); **Q**−**X$_E$** (cyan); **Q**−**X$_A$**:**Q**−**X$_B$** (purple).

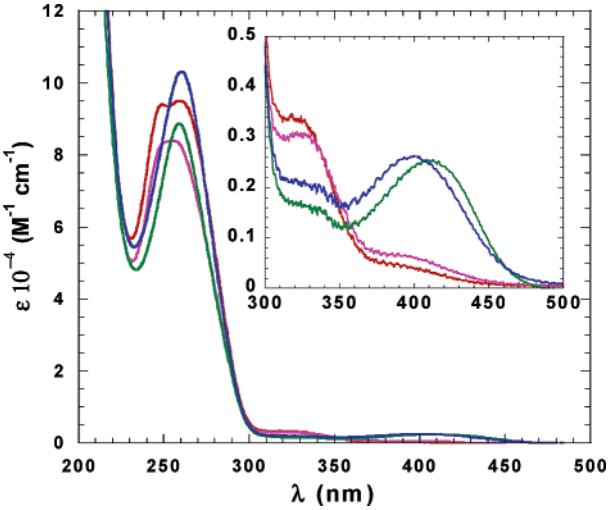


***Figure 2.*** Electronic absorption spectra of **Q**−**X$_A$**:**Q**−**X$_B$** solution at 25 °C (purple) and 95 °C (red) and of those in the presence of an equimolar amount of $CuCl_2$ at 25 °C (green) and 95 °C (blue). Solutions were prepared in pH = 7.0 10 mM phosphate buffer.

that is, to the formation of PNA duplexes from strands that contain a relatively small number of Watson−Crick base pairs. However, strong metal coordination to the ligands within the PNA strands cannot be a high enough driving force for the formation of duplexes in the absence of any Watson−Crick complementarity.

**UV−Vis Titrations.** To evaluate the influence of hydrogen-bonding association of **Q**−**PNA** strands on metal binding, we have conducted titrations at 25 and 95 °C, which are temperatures above and below $T_m$ for the duplexes formed from these strands. At both temperatures, the electronic absorption spectra of **Q**−**PNA** oligomers in pH 7.0 sodium phosphate buffer (Figure 2) are dominated by two strong absorption bands at 260 and 247 nm, which correspond to $\pi-\pi^*$ transitions of the nucleobases and of the **Q** ligand, respectively.[36−38] A shoulder at 320 nm (inset in Figure 2) is due to $\pi-\pi^*$ transitions of **Q**. At both 25 and 95 °C, the effect of $Cu^{2+}$ addition to **Q**−**X$_i$** solutions is the expected bathochromic shift of the ligand absorption band from 247 to 260, the hypochromicity of the ligand $\pi-\pi^*$ band at 320 nm, and the appearance of a metal-to-ligand charge-transfer band at ~400 nm,[39] demonstrating that $Cu^{2+}$ binds indeed to **Q** at both temperatures. To determine the stoichiometry of $Cu^{2+}$ binding to **Q**−**PNA**, we have conducted spectrophotometric titrations of **Q**−**PNA** with $Cu^{2+}$ by monitoring changes in absorbance at the above wavelengths. **Q**−**PNA** solutions with total concentrations of 10 $\mu$M (Figures 3 and 4) and 50 $\mu$M (Figures 5 and 6) were titrated with $CuCl_2$ solutions at 25 °C (Figures 3, 5, S4, S5, S7, S9) and at 95 °C (Figures 4, 6, S2, S3, S6, S8, S10, S11). The results of spectrophotometric titrations for **Q**−**X$_i$** single strands where i = A−D and for equimolar mixtures of **Q**−**X$_A$** and **Q**−**X$_B$** are similar to each other at both temperatures (Figures 3−6 and S2−S9).

At 95 °C, the UV−vis titration curves at 247, 260, 320, and 400 nm of all **Q**−**PNA** strands show a first inflection point at $Cu^{2+}$:**Q**−**X$_i$** of 1:2 (part b of Figures 4, 6, S2, S3, S6, S8, S10, and S11). Two isosbestic points are observed at 253 and 349 nm, indicating a direct conversion of **Q**−**X$_i$** to [Cu(**Q**−**X$_i$**)$_2$] (part a of Figures 4, 6, S2, S3, S6, S8, S10, and S11). Further addition of $Cu^{2+}$ leads to a second inflection point corresponding to the formation of 1:1 [Cu(**Q**−**X$_i$**)] complexes. The transformation of the 1:2 complex into a 1:1 complex is also accompanied by a hypsochromic shift ($\Delta\lambda$ = 7 nm) of the metal-to-ligand charge-transfer transition from 400 to 393 nm. The small hyperchromicity observed at 260 nm after the 1:1 complex has formed can be attributed to weak interaction of copper ions with unpaired PNA nucleobases (Figures 4b, S2b,

***Table 1.*** Melting Temperatures $T_m$ and Interactions That Affect $T_m$

| | (**Q**–**X$_A$**:**Q**–**X$_B$**)–$Cu^{2+}$ | (**Q**–**X$_B$**:**Q**–**X$_B$**)–$Cu^{2+}$ | (**Q**–**X$_C$**:**Q**–**X$_C$**)–$Cu^{2+}$ | (**Q**–**X$_A$**:**Q**–**X$_A$**)–$Cu^{2+}$ | (**Q**–**X$_D$**:**Q**–**X$_D$**)–$Cu^{2+}$ | $Cu^{2+}$(**Q**–**X$_E$**)$_2$ |
|---|---|---|---|---|---|---|
| $T_m$ | >79 | >79 | 77 | 72 | 66 | |
| Watson−Crick bp | 9 | 4 | 6 | 4 | 4 | 0 |
| wobble bp | 0 | 2 | 0 | 2 | 0 | 0 |
| overhangs | 0 | 2 A | 0 or 2 CT | 2 T | 0 or 2 CT | 2 A |

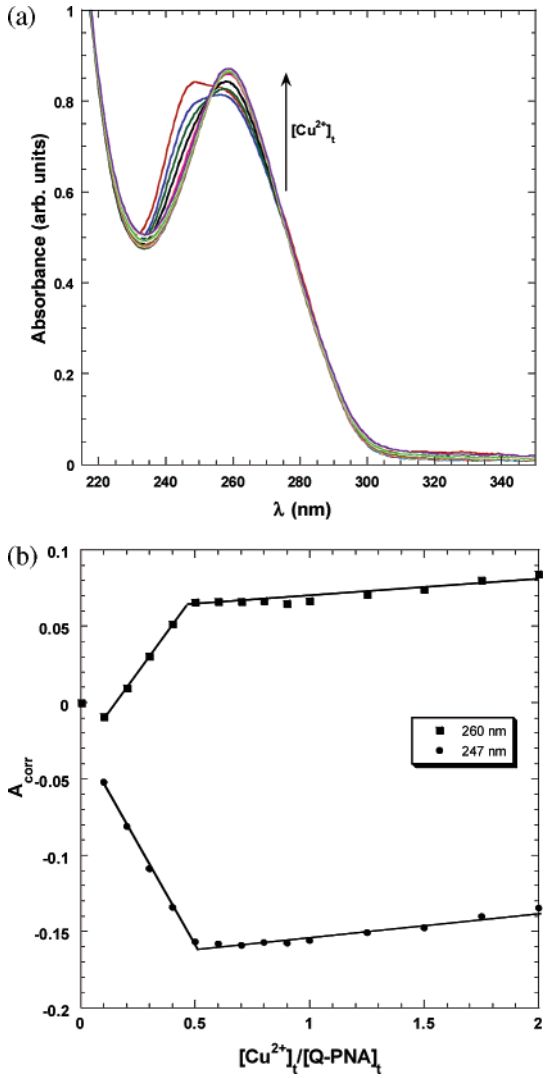


***Figure 3.*** Spectrophotometric titration of a 5 $\mu$M **Q**−**X**$_{\mathbf{A}}$ and 5 $\mu$M **Q**−**X**$_{\mathbf{B}}$ solution in pH = 7.0 10 mM phosphate buffer with 0.500 mM $CuCl_2$ solution, $T$ = 25 °C.

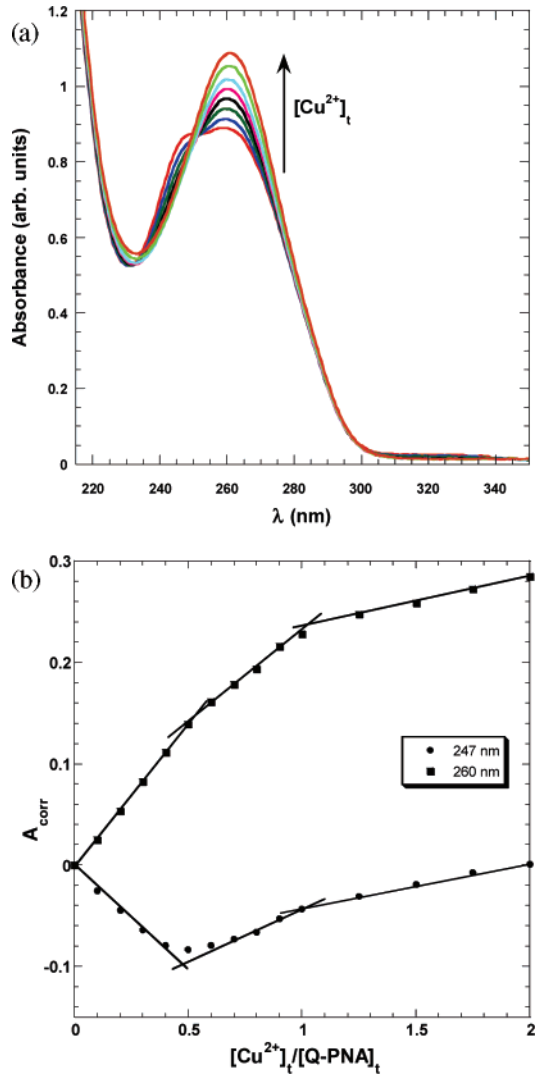


***Figure 4.*** Spectrophotometric titration of a 5 $\mu$M **Q**−**X**$_{\mathbf{A}}$ and 5 $\mu$M **Q**−**X**$_{\mathbf{B}}$ solution in pH = 7.0 10 mM phosphate buffer with 0.500 mM $CuCl_2$ solution, $T$ = 95 °C.

S8b, S15b). This hypothesis is supported by the titration of the nonmodified PNA duplex **X**$_{\mathbf{A}}$:**X**$_{\mathbf{B}}$ with $Cu^{2+}$, which shows indeed a very weak increase in absorbance at 260 nm with increasing $Cu^{2+}$ concentration (Figure S12). Furthermore, the increase in absorbance after quantitative $Cu^{2+}$ binding to **Q** ligands in the **Q**−**PNA** duplexes is significantly lower at 25 °C, where all nucleobases are involved in hydrogen bonding. The same two complexes [Cu(**Q**−**X**$_{\mathbf{B}}$)$_2$] and [Cu(**Q**−**X**$_{\mathbf{B}}$)] form in the opposite order in the reverse titration of $Cu^{2+}$ solutions with **Q**−**X**$_{\mathbf{B}}$ at 95 °C (Figures S13).

UV−vis titrations at 25 °C show two isosbestic points at 254 and 353 nm, but in contrast to the observations made at 95 °C, the changes in absorbance show a single inflection point at 2:1 **Q**−**PNA**:$Cu^{2+}$ molar ratio, indicating that once the (**Q**−**X**$_{\mathbf{i}}$:**Q**−**X**$_{\mathbf{i}}$)−$Cu^{2+}$ (i = A−D) duplexes form, they cannot be converted by excess $Cu^{2+}$ to Cu(**Q**−**X**$_{\mathbf{i}}$) complexes (Figures 3, 5, S4, S5, S7, S9, S14). Notably the charge-transfer transition that occurs at 376 nm for the synthetic Cu**Q**$_2$ is shifted to 412 nm for the (**Q**−**X**$_{\mathbf{i}}$:**Q**−**X**$_{\mathbf{i}}$)−$Cu^{2+}$ duplexes formed at 25 °C, which is likely due to steric influence exerted by the PNA duplex on the geometry of the Cu**Q**$_2$ moiety. Similar UV−vis titrations of **Q**−**X**$_{\mathbf{E}}$ with $Cu^{2+}$ show that addition of $Cu^{2+}$ leads to transformation of [Cu(**Q**−**X**$_{\mathbf{E}}$)$_2$] into [Cu(**Q**−**X**$_{\mathbf{E}}$)] not only at 95 °C (Figures S10 and S11) but also at 25 °C (Figures 7 and 8), as expected because **Q**−**X**$_{\mathbf{E}}$ cannot form a homoduplex based on Watson−Crick base pairing. The transformation of [Cu(**Q**−**X**$_{\mathbf{E}}$)$_2$] to [Cu(**Q**−**X**$_{\mathbf{E}}$)] is supported not only by the observation of two inflection points in titration curves (Figures 7b and 8b) but also by the hypsochromic shift of the 400 nm band characteristic for [Cu(**Q**−**X**$_{\mathbf{E}}$)$_2$] to 393 nm characteristic for the [Cu(**Q**−**X**$_{\mathbf{E}}$)]complex (Figure 8a).

Additionally, the transformation of [Cu(**Q**−**PNA**)$_2$] to [Cu(**Q**−**PNA**)] upon addition of excess $Cu^{2+}$ has been confirmed by titrations with 5,5′-dimethyl-2,2′-bipyridine (Me-bipy), monitored at ∼400 nm, which is a charge-transfer transition of Cu**Q**$_2$, and at 318 nm, which is an absorption band of coordinated Me-bipy. Upon Me-bipy addition to solutions that are 40 $\mu$M in $Cu^{2+}$ and 40 $\mu$M in **Q**−**X**$_{\mathbf{B}}$, besides the appearance of bands characteristic for the $Cu^{2+}$-coordinated Me-bipy at 318

(36) Philips, J. P.; Huber, W. H.; Chunga, J. W.; Merritt, L. L. *J. Am. Chem. Soc.* **1951**, *73*, 630−632.
(37) Stone, K. G.; Friedman, L. *J. Am. Chem. Soc.* **1947**, *69*, 209−211.
(38) Sone, K. *J. Am. Chem. Soc.* **1953**, *75*, 5207−5211.
(39) Amundsen, A. R.; Whelan, J.; Bosnich, B. *J. Am. Chem. Soc.* **1977**, *99*, 6730−6739.

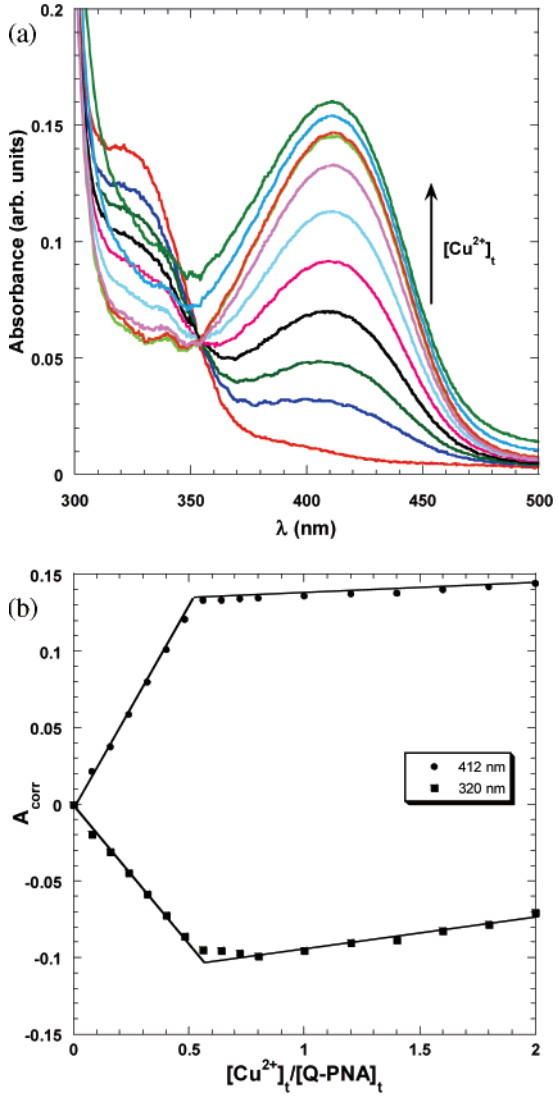


***Figure 5.*** Spectrophotometric titration of a 25 $\mu$M **Q**−**X$_A$** and 25 $\mu$M **Q**−**X$_B$** solution in pH = 7.0 10 mM phosphate buffer with 2.00 mM $CuCl_2$ solution, $T$ = 25 °C.

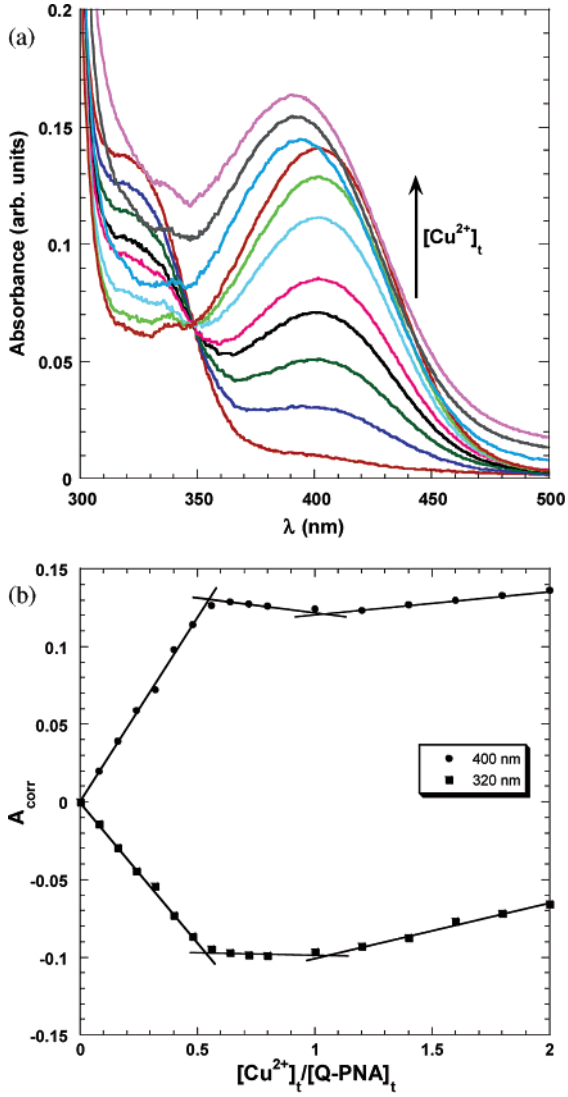


***Figure 6.*** Spectrophotometric titration of a 25 $\mu$M **Q**−**X$_A$** and 25 $\mu$M **Q**−**X$_B$** solution in pH = 7.0 10 mM phosphate buffer with 2.00 mM $CuCl_2$, $T$ = 95 °C.

nm, the charge-transfer band of the $Cu^{2+}$-coordinated 8-hydroxyquinoline moiety undergoes a bathochromic shift from 393 to 400 nm (Figure 9). The absorbance increase at 318 and at 400 nm has an inflection point at a $Cu^{2+}$:Me-bipy ratio of 1:2. The bathochromic shift and inflection point indicate that [Cu(**Q**−**X$_B$**)] ($\lambda_{max}$ = 393 nm) transforms into [Cu(**Q**−**X$_B$**)$_2$] complex ($\lambda_{max}$ = 400 nm) concomitant with formation of [Cu(Me-bipy)] ($\lambda_{max}$ = 318 nm):

$$2[\mathrm{Cu}(\mathbf{Q}-\mathbf{X_B})] + \text{Me-bipy} \rightarrow [\mathrm{Cu}(\mathbf{Q}-\mathbf{X_B})_2] + [\mathrm{Cu}(\text{Me-bipy})]$$

Titrations at 95 °C of solutions with a 1:2 Cu:**Q**−**X$_B$** ratio showed no change in the absorbance or position of the 400 nm band, indicating that the [Cu(**Q**−**X$_B$**)$_2$] complex is stable to Me-bipy addition (Figure 10).

These observations indicate that binding of 0.5 equiv of $Cu^{2+}$ to **Q** ligands leads to association of **Q**−**X$_i$** strands into [Cu(**Q**−**X$_i$**)$_2$] complexes at any temperature. Above the melting temperature, [Cu(**Q**−**X$_i$**)$_2$] are converted to [Cu(**Q**−**X$_i$**)] upon addition of $Cu^{2+}$, irrespective of the degree of (self)-complementarity of **Q**−**X$_i$** strands. The latter behavior is different from that of 8-hydroxyquinoline under the same conditions, which at 95 °C forms [Cu**Q**$_2$] complexes stable with respect to further addition of $Cu^{2+}$ (see Supporting Information, pages S8−S10). This difference is attributed to the conformational entropy loss for the complex formation, which is larger for **Q**−**PNA** strands than for 8-hydroxyquinoline itself. Comparison of the low-temperature behavior of the noncomplementary **Q**−**X$_E$** strand with the partly complementary **Q**−**X$_i$**, i = A−D, strands indicates that if the [Cu(**Q**−**X$_i$**)$_2$] complexes are held together not only by metal ion coordination bonds but also by hydrogen bonds within Watson−Crick base pairs, the enthalpic stabilization overcomes the entropic destabilization of 1:2 complexes with respect to 1:1 complexes and leads to the relationship between stepwise binding constants for $Cu^{2+}$ to **Q**−**PNA**: $K_1 \ll K_2$.

**EPR Spectroscopy.** To further investigate the coordination of $Cu^{2+}$ to **Q**−**PNA**, we have recorded EPR spectra for solutions containing duplexes annealed in the presence of $Cu^{2+}$. In the presence of phosphate anions, $Cu^{2+}$ forms EPR-silent, polynuclear complexes. Thus, for our samples that are prepared in phosphate buffer, an EPR spectrum is expected only if the

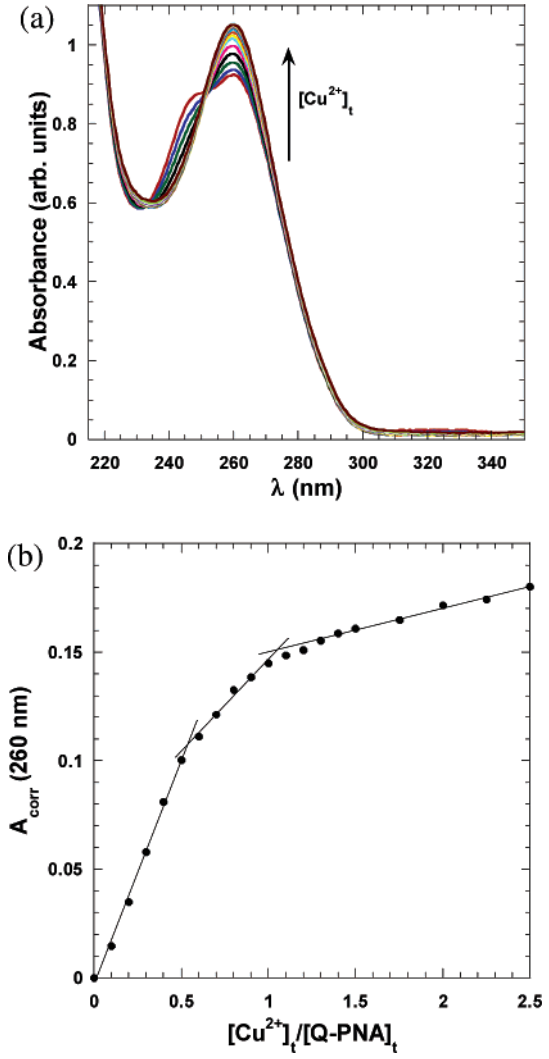


***Figure 7.*** Spectrophotometric titration of a 10 $\mu$M **Q**−$\mathbf{X_E}$ solution in pH = 7.0 10 mM phosphate buffer with 0.500 mM $CuCl_2$ solution, $T$ = 25 °C.

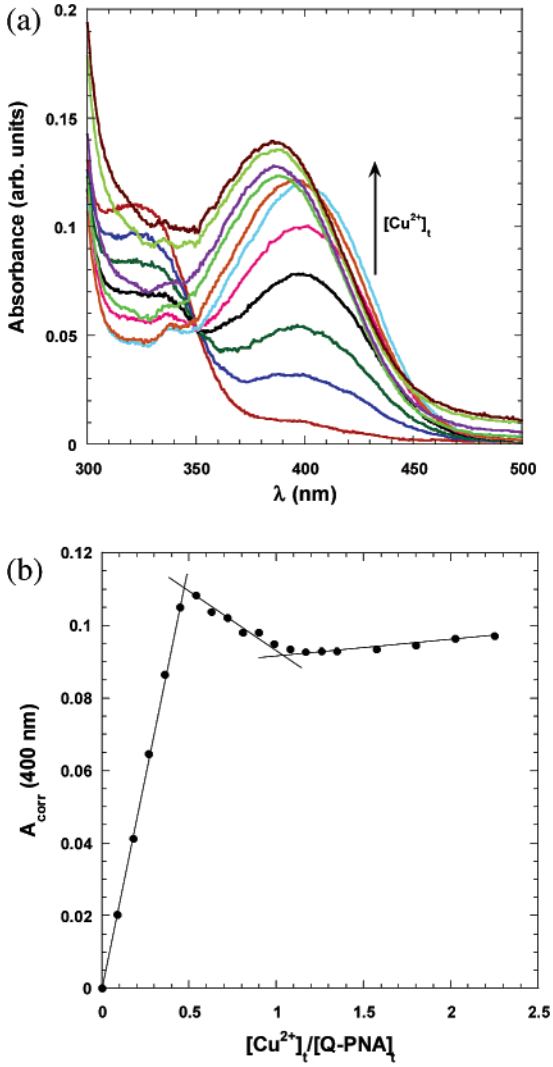


***Figure 8.*** Spectrophotometric titration of a 40 $\mu$M **Q**−$\mathbf{X_E}$ solution in pH = 7.0 10 mM phosphate buffer with 2.00 mM $CuCl_2$ solution, $T$ 25 °C.

phosphate complexes are destroyed by binding of $Cu^{2+}$ to stronger ligands in the modified **Q**−**PNA**. Indeed, a 100 $\mu$M $Cu^{2+}$ solution in pH 7.0 sodium phosphate buffer showed a very weak EPR spectrum, which integrated to <5 $\mu$M $Cu^{2+}$. No spectrum was observed for the duplex $\mathbf{X_A}$:$\mathbf{X_B}$ formed by annealing in the presence of $Cu^{2+}$, which confirms that at this concentration level $Cu^{2+}$ does not bind to the nucleobases involved in hydrogen bonding within the Watson−Crick base pairs.

EPR spectra for solutions of duplexes that contain 8-hydroxyquinoline ligands, (**Q**−$\mathbf{X_A}$:**Q**−$\mathbf{X_A}$)−$Cu^{2+}$, (**Q**−$\mathbf{X_B}$:**Q**−$\mathbf{X_B}$)−$Cu^{2+}$, (**Q**−$\mathbf{X_C}$:**Q**−$\mathbf{X_C}$)−$Cu^{2+}$, and (**Q**−$\mathbf{X_A}$:**Q**−$\mathbf{X_B}$)−$Cu^{2+}$, were similar to each other and indicative of $Cu^{2+}$ coordinated to the **Q** ligands (Figure 11). Simulation of the EPR spectra with an $S = {}^1/_2$ spin Hamiltonian that includes hyperfine parameters for $^{63,65}Cu^{2+}$ ($I = {}^3/_2$) and $^{14}N$ ($I = 1$) leads to parameters (Table 2) similar to those measured for the [Cu$\mathbf{Q}_2$] complex in toluene/chloroform solutions or in pH 8.5 ethylene glycol−water glasses and confirms binding of $Cu^{2+}$ to two **Q** ligands.[40,41] The small difference between the $A_3$ values for the PNA-incorporated [Cu$\mathbf{Q}_2$] and for the synthetic complex may be due to weak interactions between the adjacent base pairs and the $Cu^{2+}$ ion coordinated to two **Q** ligands, as previously observed by Atwell et al.,[42] to weak binding of water or phosphate molecules in the axial positions of the complex, or to differences between the structure of the free- and PNA-enclosed-[Cu$\mathbf{Q}_2$] moiety. Integration of the EPR signals for all homoduplexes and for (**Q**−$\mathbf{X_A}$:**Q**−$\mathbf{X_B}$)−$Cu^{2+}$ confirmed the quantitative 1:2 binding of $Cu^{2+}$ to the two 8-hydroxyquinoline ligands present within the ligand-containing duplexes, in agreement with the results of spectrophotometric titrations.

**CD Spectroscopy.** Having obtained from UV−vis and EPR spectroscopy information about the $Cu^{2+}$ coordination to **Q**−**PNA**, we have used CD spectroscopy to investigate the secondary structure of the duplexes formed upon metal binding. In contrast to DNA, which has a chiral backbone and shows a CD spectrum characteristic for each type of duplex (e.g., A, B, or Z), PNA has an achiral backbone and PNA duplexes show a preference for a given handedness only upon chiral induction by an enantiomerically pure component, such as an L-amino acid attached to the carboxy terminus of the PNA oligomers.[34,43]

(40) Walker, F. A.; Sigel, H.; McCormick, D. B. *Inorg. Chem.* **1972**, *11*, 2756−2763.
(41) Gersmann, H. R.; Swalen, J. D. *J. Chem. Phys.* **1962**, *36*, 3221−3233.
(42) Atwell, S.; Meggers, E.; Spraggon, G.; Schultz, P. G. *J. Am. Chem. Soc.* **2001**, *123*, 12364−12367.

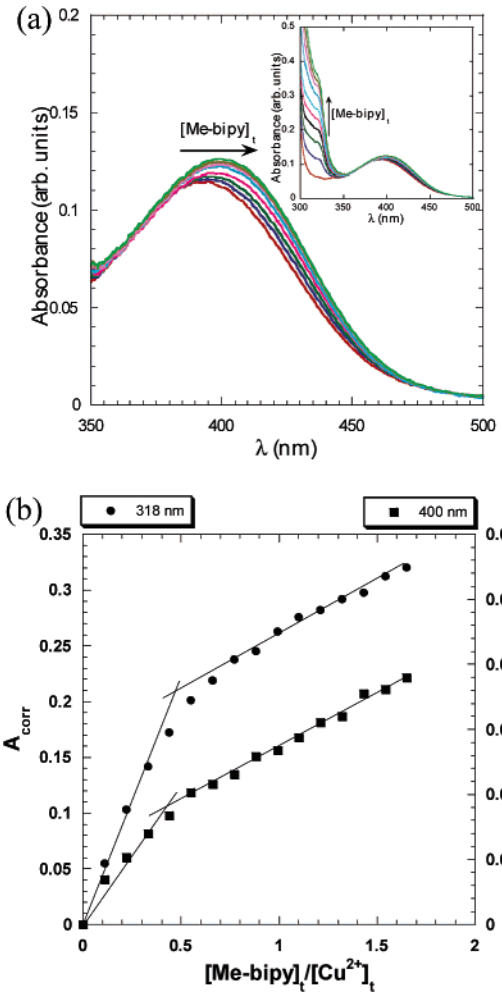


***Figure 9.*** Spectrophotometric titration of a 40 $\mu$M $CuCl_2$ and 40 $\mu$M **Q**−$\mathbf{X_B}$ solution with a 2.00 mM Me-bipyridine solution in pH = 7.0 10 mM phosphate buffer, $T$ = 95 °C (inset: view of absorbance for 300 < $\lambda$ < 500 nm).

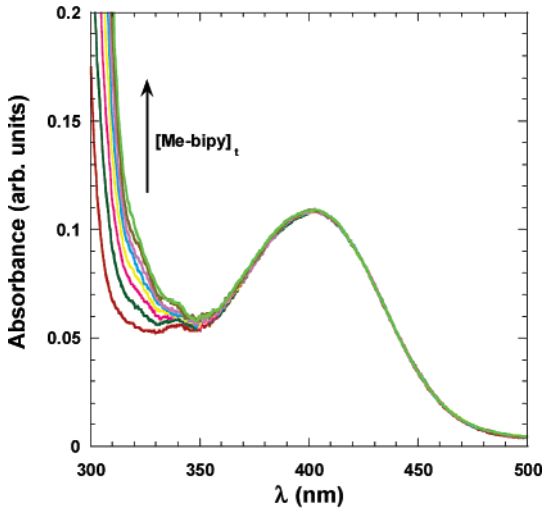


***Figure 10.*** Spectrophotometric titration of a 20 $\mu$M $CuCl_2$ and 40 $\mu$M **Q**−$\mathbf{X_B}$ solution with a 2.00 mM Me-bipyridine solution in pH = 7.0 10 mM phosphate buffer, $T$ = 95 °C.

The chiral induction effect depends on the type of base pair that is adjacent to the chiral component of the PNA duplex, with the more stable GC base pair being more efficient in transmitting the effect than an AT pair.[43] On the basis of this observation, one would predict that mismatches and coplanar metal-coordinated ligand pairs have a negative and positive impact, respectively, on the chirality of modified PNA duplexes, a hypothesis supported by our experimental results.

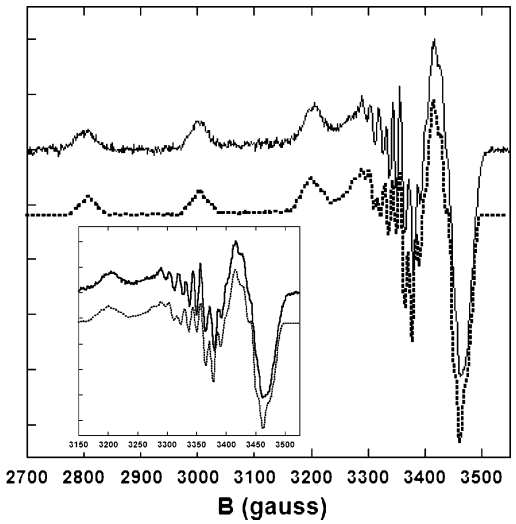


***Figure 11.*** Perpendicular mode X-band EPR spectrum of a 100 $\mu$M (**Q**−$\mathbf{X_A}$:**Q**−$\mathbf{X_B}$)−Cu solution in pH 7.0 10 mM sodium phosphate buffer with 25% glycerol (solid line) and simulation (dotted line) using the parameters given in Table 2. $T$ = 20 K, frequency 9.65 GHz, microwave power 0.02 mW, modulation amplitude 6.676 G.

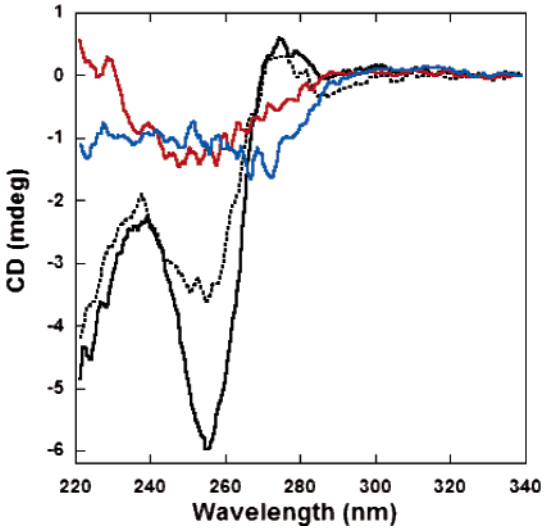


***Figure 12.*** CD spectra of annealed 20 $\mu$M **Q**−$\mathbf{X_A}$ (red) and 20 $\mu$M **Q**−$\mathbf{X_B}$ (blue), and 10 $\mu$M **Q**−$\mathbf{X_A}$:**Q**−$\mathbf{X_B}$ in the absence (black dotted line) and in the presence (black solid line) of 10 $\mu$M $Cu(NO_3)_2$. Solutions were prepared in pH 7.0 10 mM sodium phosphate buffer.

We have measured the CD spectra of **Q**-modified PNA homoduplexes [**Q**−$\mathbf{X_A}$:**Q**−$\mathbf{X_A}$] and [**Q**−$\mathbf{X_B}$:**Q**−$\mathbf{X_B}$] in the absence and presence of $Cu^{2+}$ and found that they do not show a preferred handedness (Figure 12). The heteroduplex **Q**−$\mathbf{X_A}$:**Q**−$\mathbf{X_B}$ has a preferred left-handedness in the absence of $Cu^{2+}$, which coincides with that of the nonmodified PNA duplex.[44,45] (**Q**−$\mathbf{X_A}$:**Q**−$\mathbf{X_B}$)−$Cu^{2+}$ has a significantly more intense CD spectrum than that of the **Q**−$\mathbf{X_A}$:**Q**−$\mathbf{X_B}$ duplex

(43) Wittung, P.; Eriksson, M.; Lyng, R.; Nielsen, P. E.; Norden, B. *J. Am. Chem. Soc.* **1995**, *117*, 10167−10173.
(44) Sforza, S.; Haaima, G.; Marchelli, R.; Nielsen, P. E. *Eur. J. Org. Chem.* **1999**, 197−204.
(45) Lagriffoule, P.; Wittung, P.; Eriksson, M.; Jensen, K. K.; Norden, B.; Buchardt, O.; Nielsen, P. E. *Chem.-Eur. J.* **1997**, *3*, 912−919.

***Table 2.*** EPR Parameters for [Cu$\mathbf{Q}_2$] within the PNA Context and in the Synthetic Complex[a]

| | (**Q**–$\mathbf{X_A}$:**Q**–$\mathbf{X_B}$)–$Cu^{2+}$ | (**Q**–$\mathbf{X_A}$:**Q**–$\mathbf{X_A}$)–$Cu^{2+}$ | (**Q**–$\mathbf{X_B}$:**Q**–$\mathbf{X_B}$)–$Cu^{2+}$ | [Cu$\mathbf{Q}_2$][40] | (**G**:**G**)–$Cu^{2+}$ |
|---|---|---|---|---|---|
| $g_1$ | 2.06 | 2.06 | 2.06 | 2.06 | 2.07 |
| $g_2$ | 2.05 | 2.05 | 2.05 | 2.06 | 2.07 |
| $g_3$ | 2.22 | 2.22 | 2.23 | 2.24 | 2.32 |
| $A_1$ (MHz) | 72 | 73 | 69 | 72 | |
| $A_2$ (MHz) | 80 | 80 | 79 | 72 | |
| $A_3$ (MHz) | 611 | 612 | 607 | 530 | 486 |
| $A_{1N}$ (MHz) | 39 | 39 | 39 | 39 | |
| $A_{2N}$ (MHz) | 32 | 31 | 34 | 33 | |
| $A_{3N}$ (MHz) | 36 | 35 | 37 | 33 | |

[a] $A_i$ and $A_{iN}$ are hyperfine coupling constants for copper and nitrogen nuclei, respectively.

(Figure 12), which suggests that despite being situated far from the chiral, C-terminal amino acid, the metal−ligand pair significantly influences the transmission of the chiral effect through the duplex. On the other hand, even in the presence of $Cu^{2+}$, no chiral excess is induced by the L-lysine residue in **Q**−$\mathbf{X_A}$:**Q**−$\mathbf{X_A}$ and **Q**−$\mathbf{X_B}$:**Q**−$\mathbf{X_B}$ duplexes, which have a significantly lower number of hydrogen-bonded base pairs. This observation reinforces the idea that $\pi$-stacking interactions throughout the duplex are an important condition for transmission of the chiral effect.[34,43]

Given the intense CD signal at 256 nm of **Q**−$\mathbf{X_A}$:**Q**−$\mathbf{X_B}$ and (**Q**−$\mathbf{X_A}$:**Q**−$\mathbf{X_A}$)−$Cu^{2+}$, we have also performed thermal denaturation studies by monitoring the CD intensity at this wavelength and found good agreement with the melting curves measured using UV hypochromicity (Figure S19).

## Discussion

EPR spectroscopy and spectrophotometric titrations measure the stoichiometry of complexes formed between $Cu^{2+}$ and **Q**−**PNA** and show that, in solutions containing a $Cu^{2+}$:**Q**−**PNA** ratio of 1:2, [Cu(**Q**−$\mathbf{X_i}$)$_2$] complexes form irrespective of the nucleobase sequence of the ligand-containing PNA strands **Q**−$\mathbf{X_i}$ and of the temperature. The similarity between the UV−vis and EPR spectra for the synthetic [Cu$\mathbf{Q}_2$] complex known to adopt a four-coordinate, square planar coordination and for (**Q**−$\mathbf{X_i}$:**Q**−$\mathbf{X_i}$)−$Cu^{2+}$ duplexes indicates that the copper coordination in the duplexes is also square planar. The small difference between the $A_3$ values for these compounds could be due to binding of one or two more ligands in axial positions to $Cu^{2+}$ or to differences between the geometry of the [Cu$\mathbf{Q}_2$] unit in the synthetic complex and that in the PNA-bound one. Coordination of a single water molecule to $Cu^{2+}$ is unlikely because, as observed in the crystal structure of the five-coordinate complex [Cu$\mathbf{Q}_2$($OH_2$)], the planes of the aromatic rings of the two **Q** ligands would form a 50° dihedral angle, an arrangement which would have a destabilization rather than a stabilization effect on the PNA duplex.[46−48] Examination of the crystal structure of a six-coordinate [Cu$\mathbf{Q}_2$($OH_2$)$_2$] complex shows that the axial Cu−$O_{H_2O}$ distances are 2.45 Å and that the complexes are arranged in the crystal in stacks of parallel-oriented molecules with the distance between the planes of adjacent molecules being 5.54 Å.[49] Based on these observations, the binding of two extraneous small ligands (e.g., water or phosphate) to the [Cu$\mathbf{Q}_2$] moiety within PNA is unlikely because it would require significant distortions of the duplex to accommodate the axial ligands of $Cu^{2+}$. It is also notable that the intermolecular distance between stacked [Cu$\mathbf{Q}_2$] molecules in single crystals is 3.36 Å, which is similar to the distance between natural base pairs in PNA duplexes.[50,51] If indeed the differences in the EPR values are due to weak binding of axial ligands, these ligands would have to be nucleobases adjacent to the [Cu$\mathbf{Q}_2$] site, as previously observed by Atwell et al.[42] Additionally, while all structurally characterized, four-coordinate synthetic complexes of $Cu^{2+}$ with two 8-hydroxyquinoline have a trans arrangement of the ligands,[24−27] we cannot rule out a cis orientation of the two **Q** ligands within the PNA duplex, and such an orientation could also lead to differences between the EPR spectra of the **Q**−**PNA** duplexes and of the synthetic complex. This orientation has been proposed by Zhang et al.,[14] but no experimental evidence was brought forth. For the cis isomer, the relative orientation of the C−C bonds that link the 8-hydroxyquinoline to the PNA or DNA backbone is closer to that of the C−C bonds that link GC and AT base pairs to the duplex backbone than the relative orientation for a trans isomer. On the other hand, a cis orientation of the two 8-hydroxyquinoline within a square planar complex leads to a steric clash between the protons situated on the $C_2$ atoms of the ligand, which could lead to tetrahedral distortion of the complex and weakening of the H bonds of the bases adjacent to the Cu$\mathbf{Q}_2$ moiety. We are currently pursuing combined electronic structure and molecular modeling calculations to evaluate these possibilities.

Variable-temperature UV spectroscopy shows that full Watson−Crick complementarity is not necessary for the formation of metal-bridged duplexes. Solutions of **Q**−**PNA** strands that contain one 8-hydroxyquinoline and have as few as four complementary base pairs form in the presence of 0.5 equiv of $Cu^{2+}$ duplexes that show a cooperative melting transition. This transition takes place with significant hyperchromicity, and $T_m$ can be correlated with the degree of self-complementarity of the **Q**−$\mathbf{X_i}$ single strands. The fully complementary strands **Q**−$\mathbf{X_A}$ and **Q**−$\mathbf{X_B}$ form the duplex (**Q**−$\mathbf{X_A}$:**Q**−$\mathbf{X_B}$)−$Cu^{2+}$, which has the highest thermal stability, while the noncomplementary strand **Q**−$\mathbf{X_E}$ does not form a stable duplex despite the fact that $Cu^{2+}$ leads to association of the strands into [Cu(**Q**−$\mathbf{X_E}$)$_2$] complexes. In contrast, the partially complemen-

(46) Jian, F.; Wang, Y.; Lu, L.; Yang, X.; Wang, X.; Chantrapromma, S.; Fun, H. K.; Razak, I. A. *Acta Crystallogr., Sect. C* **2001**, *57*, 714−716.
(47) Kruh, R.; Dwiggins, C. W. *J. Am. Chem. Soc.* **1955**, *77*, 806.
(48) Suito, E.; Arakawa, M.; Kobayashi, T. *Kolloid Z. Z. Polym.* **1966**, *212*, 155−161.
(49) Okabe, N.; Saishu, H. *Acta Crystallogr., Sect. E* **2001**, *57*, m251−m252.
(50) Petit, S.; Coquerel, G.; Perez, G.; Louer, D.; Louer, M. *Chem. Mater.* **1994**, *6*, 116−121.
(51) Petersson, B.; Nielsen, B. B.; Rasmussen, H.; Larsen, I. K.; Gajhede, M.; Nielsen, P. E.; Kastrup, J. S. *J. Am. Chem. Soc.* **2005**, *127*, 1424−1430.

tary homoduplexes ($\mathbf{Q-X_i}$:$\mathbf{Q-X_i}$)$-Cu^{2+}$ have intermediate thermal stability (c−f in Chart 1). In Chart 1, all duplexes are written with their strands in antiparallel alignment and with the Q ligands placed in complementary positions. In these alignments, no Watson−Crick base pair would form in duplexes $\mathbf{Q-X_C}$:$\mathbf{Q-X_C}$ and $\mathbf{Q-X_D}$:$\mathbf{Q-X_D}$, and their stability would be expected to be low. In contrast, arrangements shown in Chart 2 for the $\mathbf{Q-X_C}$:$\mathbf{Q-X_C}$ and $\mathbf{Q-X_D}$:$\mathbf{Q-X_D}$ duplexes lead to six and four Watson−Crick base pairs, respectively, and place the two **Q** ligands of each duplex in close proximity to each other. The EPR spectrum of the ($\mathbf{Q-X_C}$:$\mathbf{Q-X_C}$)$-Cu^{2+}$ duplex and the spectrophotometric titration at 25 °C (Figure S9) of $\mathbf{Q-X_D}$:$\mathbf{Q-X_D}$ with $Cu^{2+}$ establishes coordination of one $Cu^{2+}$ to two **Q** ligands per duplex.[52] To allow the formation of the $Cu\mathbf{Q}_2$ moiety in these duplexes, the bases across from the two **Q** ligands can either be situated within the duplex and have $\pi-\pi$ interactions with the adjacent base pairs or be bulged out of the duplex. Table 1 shows the $T_m$'s for all homoduplexes as well as the maximum number of Watson−Crick and wobble base pairs and the number and type of overhangs of each duplex. Analysis of the data contained in the table indicates a correlation between the number of complementary base pairs in each duplex and its $T_m$. Duplex ($\mathbf{Q-X_C}$:$\mathbf{Q-X_C}$)$-Cu^{2+}$, which can form six Watson−Crick base pairs, is more stable than homoduplexes A, B, D, which can form at most four Watson−Crick base pairs. For duplexes ($\mathbf{Q-X_i}$:$\mathbf{Q-X_i}$)$-Cu^{2+}$, where i = B, A, and D, the thermal stability increases if besides the four Watson−Crick base pairs they can either form two additional wobble base pairs (i.e., duplexes with i = A or B) or contain overhang bases, with A overhangs having a larger stabilization effect than T overhangs as previously observed in PNA duplexes[53] (compare ($\mathbf{Q-X_B}$:$\mathbf{Q-X_B}$)$-Cu^{2+}$ with ($\mathbf{Q-X_A}$:$\mathbf{Q-X_A}$)$-Cu^{2+}$ and ($\mathbf{Q-X_D}$:$\mathbf{Q-X_D}$)$-Cu^{2+}$ in Charts and in Table 1).

Formation of PNA duplexes even from partly complementary PNA strands can be rationalized by assuming that the tight binding of the two strands by $Cu^{2+}$ coordination to the ligands centrally located in the PNA strands overcomes the loss of translational entropy for the duplex formation and brings the nucleobases in sufficient proximity such that $\pi-\pi$ interactions and a few hydrogen bonds are a sufficient driving force for duplex formation.[54] The noncomplementary bases within the duplexes formed from partly complementary **Q−PNA** strands are likely involved in $\pi-\pi$ stacking interactions within the duplex, as indicated by the high hypochromicity observed in the melting curves. A related effect of zipper-like recognition based on interstrand $\pi$-stacking interactions has been reported by Brotschi et al.[55,56] In a study of DNA duplexes containing hydrophobic biphenyl (Bph) residues instead of nucleobases, they have shown that an increasing number of Bph moieties situated in the middle of a DNA duplex leads to an increase of the $T_m$ as measured by monitoring hypochromicity at 260 nm.[55] The CD spectra of the DNA duplexes containing up to eight Bph residues did not differ from those of the corresponding nonmodified DNA duplexes, which suggests that the Bph residues adopt a highly ordered, stacked arrangement within the double helix. It is notable that in contrast to the biphenyl-modified DNA in which complementary natural base pairs flank the biphenyl residues situated in the middle of the PNA duplex, in the PNA system under consideration in the present paper, interactions of the natural base pairs at the extremities of the duplex are triggered by strong binding between the metal ion and the ligands situated in the middle of the duplex.

At temperatures above $T_m$ and in the absence of complementarity of PNA strands, addition of excess $Cu^{2+}$ leads to conversion of [Cu($\mathbf{Q-PNA}$)$_2$] complexes to [Cu($\mathbf{Q-PNA}$)]. This transformation does not occur at 25 °C if the $Cu\mathbf{Q}_2$ moiety is situated in a PNA duplex, because the duplex exerts a supramolecular chelate effect, prearranging the ligands in close proximity and making the stability of the square planar [$Cu\mathbf{Q}_2$] complex exceptionally high.

Chiral induction by L-Lys is observed only for the fully complementary ($\mathbf{Q-X_A}$:$\mathbf{Q-X_B}$)$-Cu^{2+}$ and $\mathbf{Q-X_A}$:$\mathbf{Q-X_B}$ duplexes. Norden et al. determined that the correlation length in PNA is around 10 base pairs; that is, for PNA hairpins, the CD amplitude increases almost linearly with the number of complementary base pairs of the stem up to 10 pairs, while in the case of intermolecular duplexes, the CD amplitude also increases with the duplex length up to 10 base pairs, although to a smaller extent. Notably, even if heteroduplexes ($\mathbf{Q-X_A}$:$\mathbf{Q-X_B}$)$-Cu^{2+}$ and $\mathbf{Q-X_A}$:$\mathbf{Q-X_B}$ differ only by the presence and absence, respectively, of one central [$Cu\mathbf{Q}_2$] moiety, the amplitude of their CD spectra differs by almost a factor of 2. The significantly larger intensity of the CD spectrum for ($\mathbf{Q-X_A}$:$\mathbf{Q-X_B}$)$-Cu^{2+}$ when compared to that of $\mathbf{Q-X_A}$:$\mathbf{Q-X_B}$ supports the idea that $\pi$-interactions throughout the duplex are significantly stronger upon metal binding to the **Q−PNA** duplexes, and thus the chiral effect of the Lys residue is better transmitted in the former, metal-containing duplex. The strong effect of the metal ion on the CD spectra and, implicitly, on the helicity of the duplex suggests that the correlation length may be longer for PNA duplexes that contain metal−ligand alternative base pairs, a possibility that will be investigated in future studies.

This study demonstrates that incorporation of a strong metal−ligand moiety within a PNA duplex has a strong stabilization effect on duplexes and that PNA duplexes able to form strong metal-based pairs have high tolerance to mismatches. A similar

(52) For 25 °C UV titrations of $\mathbf{Q-X_D}$ with $Cu^{2+}$, an inflection point occurs in the absorbance change of the $\pi-\pi^*$ transition of 8-hydroxyquinoline at a $\mathbf{Q-X_D}$:$Cu^{2+}$ ratio of 2:1. This observation rules out the possibility that two $Cu^{2+}$ ions would bind to the two mixed-ligand, 8-hydroxyquinoline-nucleobase coordination sites that can form within the duplex in arrangements 2 and 3 of Chart 2. Thus, if two $\mathbf{Q-X_D}$ strands are aligned to form a $\mathbf{Q-X_D}$:$\mathbf{Q-X_D}$ duplex with maximum number of Watson−Crick base pairs, which is four, one $Cu^{2+}$ must bind to the two Q ligands situated in close proximity but not in complementary positions (Chart 2). To further verify the binding ability of a **Q**−G motif, we have prepared the PNA duplex $\mathbf{G-X_A}$:$\mathbf{Q-X_B}$ = H−GTAGGTCACT−Lys−$NH_2$:$H_2N$−Lys−CATCQAGTGA−H. The EPR spectrum of the ($\mathbf{G-X_A}$:$\mathbf{Q-X_B}$)$-Cu^{2+}$ duplex is similar to that of the ($\mathbf{Q-X_A}$:$\mathbf{Q-X_B}$)$-Cu^{2+}$ duplex, indicating that one $Cu^{2+}$ is coordinated by two Q ligands. As we have ruled out the possibility that the presence of $Cu^{2+}$ would lead to the formation of ($\mathbf{Q-X_B}$:$\mathbf{Q-X_B}$)$-Cu^{2+}$ because the thermal denaturation curves do not show a $T_m$ of 79 °C characteristic for this duplex, $Cu^{2+}$ must bridge $\mathbf{G-X_A}$:$\mathbf{Q-X_B}$ duplexes to achieve a coordination of two 8-hydroxyquinoline ligands. Finally, attempts to do 25 °C spectrophotometric titrations of $\mathbf{G-X_A}$:$\mathbf{Q-X_B}$ with $Cu^{2+}$ failed because upon addition of small amounts of $Cu^{2+}$ the UV absorbance changes with time due to an increase in the background, which is indicative of scattering due to PNA aggregation and supports the idea that inter-duplex $Cu\mathbf{Q}_2$ bridges form instead of $Cu^{2+}$ coordinating a G nucleobase and a **Q** ligand within the duplex.

(53) Datta, B.; Armitage, B. A. *J. Am. Chem. Soc.* **2001**, *123*, 9612−9619.

(54) This hypothesis is supported by the fact that in the absence of $Cu^{2+}$ all partly complementary **Q−PNA** strands show very weakly cooperative thermal denaturation curves with $T_m$'s < 45 °C (Figure S20), even if the same number of Watson−Crick base pairs as in the presence of $Cu^{2+}$ could be formed.

(55) Brotschi, C.; Leumann, C. J. *Angew. Chem., Int. Ed.* **2003**, *42*, 1655−1658.

(56) Brotschi, C.; Häberli, A.; Leumann, C. J. *Angew. Chem., Int. Ed.* **2001**, *40*, 3012−3014.

stabilization effect of $Cu^{2+}$−**Q** coordination has been observed by Zhang et al. in **Q**−DNA duplexes, where it was exploited to introduce drastic changes to the backbone. In the absence of metal ions, such a backbone modification would impose an energetic penalty too high for duplex formation.[14] Interestingly, the shape of the melting curve measured by Zhang et al. for **Q**−DNA in the presence of $Cu^{2+}$ is similar to that measured for **Q**−**PNA**, which suggests that the metal−ligand moiety is the major determinant of the properties of the nucleic acid in which it is incorporated.

The potential for nanotechnology applications of metal-containing nucleic acid structures has been recognized in the past 5 years.[11,16] The results presented in this paper indicate that the presence of strongly bound metal−ligand moieties makes possible formation of nucleic acid-based structures even in the presence of a small number of Watson−Crick base pairs of natural nucleobases, a principle that can be exploited in the design and synthesis of hybrid nucleic acid−metal structures with new topologies and properties.

**Acknowledgment.** We are grateful to the National Science Foundation (CHE-0347140) and the Camille and Henry Dreyfus Foundation for financial support of this research. We thank Dr. Michael Hendrich for the EPR simulation software. NMR spectra were recorded on instruments purchased with an NSF grant (CHE-0130903). MALDI-TOF and ES mass spectrograms were recorded in the Center for Molecular Analysis at Carnegie Mellon University, which is supported by NSF grants CHE-9808188 and DBI-9729351.

**Supporting Information Available:** Absorption spectra at 25 and 95 °C for solutions containing the 8-hydroxyquinoline PNA monomer **1** and $Cu^{2+}$, spectrophotometric titrations of single strand $\mathbf{Q-X_i}$ (i = A, B, D, E) and $\mathbf{X_A}$:$\mathbf{X_B}$ with $Cu^{2+}$, spectrophotometric titration of $Cu^{2+}$ solution with $\mathbf{Q-X_B}$, spectrophotometric titration of 8-hydroxyquinoline, and titrations with Me-bipy. This material is available free of charge via the Internet at http://pubs.acs.org.

JA051336H